



ELSEVIER

Contents lists available at ScienceDirect

Optics Communications

journal homepage: [www.elsevier.com/locate/optcom](http://www.elsevier.com/locate/optcom)

# Experimental investigation of photonic microwave switching based on XGM in a SOA

Dan Zhu, Huan Wu, Shilong Pan\*

Key Laboratory of Radar Imaging and Microwave Photonics, Ministry of Education, College of Electronic and Information Engineering, Nanjing University of Aeronautics and Astronautics, Nanjing 210016, China

## ARTICLE INFO

### Article history:

Received 19 January 2015

Received in revised form

1 August 2015

Accepted 3 August 2015

### Keywords:

Radio frequency photonics

Semiconductor optical amplifiers

Switching

## ABSTRACT

The photonic microwave switching performances based on the cross gain modulation (XGM) effect in a semiconductor optical amplifier (SOA) are experimentally investigated. The influences of the key parameters of the system, such as the optical power of the pump and probe signals, the SOA bias current and the modulation depth are experimentally studied and analyzed to optimize the system performance. Important performances of the linearity, the dynamic range and the polarization sensitivity of the photonic microwave switching system are analyzed and discussed. The channel uniformities are also investigated according to the requirements of the photonic microwave switching applications.

© 2015 Elsevier B.V. All rights reserved.

## 1. Introduction

Radio frequency (RF) switches are used extensively in microwave systems to realize signal routing, function switching or system reconfiguration [1–5]. Conventionally, the RF switches are realized in the electrical domain, which always have limited bandwidth, slow switching speed and poor isolation. Thanks to the advantages of the photonic technologies in terms of wide bandwidth, flat response and immunity to electromagnetic interference, switching of RF signals in the optical domain can possibly overcome the electronic limitations. Especially, the integrated microwave devices are very promising for the switching application because of their potential to reduce mass and size [6–8]. Although many different types of photonic switches were developed for digital optical communications in the past two decades [9–12], most of them cannot be directly used for the switching of RF signals because the photonic microwave switching has different system indicators, such as switching efficiency, noise level, linearity and dynamic range [1–4]. In addition, channel uniformity of the photonic microwave switches is of critical importance for arrayed or parallel RF systems.

Previously, several techniques have been proposed and demonstrated to achieve the photonic microwave switching. One widely-adopted scheme is the photonic switch matrix [1,13–15]. A micro-electro-mechanical system (MEMS) based photonic crossbar switch is used in [1] to realize the dynamically changing of the functions of radar, communication, and electronic warfare.

Linearity and dynamic range can be guaranteed to direct the RF signals to the transmit array antenna quadrants corresponding to different functions. However, the switching time of the MEMS-based switch is limited. A time-domain switched radio-over-fiber (RoF) network is realized by using a semiconductor optical amplifier (SOA) based switching matrix, which achieves the on- and off- states via simply control of the bias currents of the SOAs [14,15]. Only very small additional penalty is introduced by the switches. But a huge number of SOAs must be applied for a switching matrix, making the system complicated, costly and power consuming.

Photonic switching of RF signals can also be accomplished based on the nonlinear effects such as cross-gain modulation (XGM), cross-phase modulation (XPM) and four-wave mixing (FWM) in SOAs [16–21]. Among them, the switching based on FWM effect has the feature of modulation-format and bit-rate transparency, and the switching speed is fast. However, the switching efficiency decreases fast with the increasing of the wavelength spacing of the pump and probe. The photonic switching based on XPM effect in SOA has an improved extinction ratio, but the system is complex since an interferometric structure must be applied [20]. The XGM effect has shown to be useful for photonic microwave switching to have relatively high switching efficiency and compact structure [22]. But the channel uniformity, which is very important for array system applications, has not been comprehensively investigated. Therefore, it is necessary to investigate the performance especially the channel uniformity of the photonic microwave switches, as the results would be an important guidance for the application of this kind of switches in practical system.

\* Corresponding author.

E-mail address: [pans@ieec.org](mailto:pans@ieec.org) (S. Pan).

In this paper, the performance, especially the channel uniformity, of the photonic microwave switching based on the XGM effect in a SOA is experimentally investigated. Parameters such as the optical powers of the pump and probe signals, the bias current of the SOA and the modulation depth of the pump signal are adjusted to optimize the system performance. Polarization sensitivity, linearity and dynamic range of the XGM-based photonic microwave switch are experimentally analyzed and discussed. The channel uniformity of the photonic switching of RF signals for both up- and down- converted signals are also investigated.

## 2. Experimental setup

The schematic diagram of the photonic switching of RF signals based on the XGM effect in a SOA is shown in Fig. 1. A lightwave with a frequency of  $\omega_{\text{pump}}$  from the pump laser diode (LD) is modulated by an RF data at a Mach-Zehnder modulator (MZM). The modulated pump signal is then coupled with a continuous-wave probe light with a frequency of  $\omega_{\text{probe}}$  and injected into a nonlinear SOA through an optical isolator. In the SOA, XGM is utilized to realize the wavelength conversion, i.e. the RF data in the pump signal is copied to the probe. By adjusting the wavelength of the probe to be in consistency with one channel of an optical wavelength division multiplexer (WDM), the RF signal brought by the optical carrier at  $\omega_{\text{probe}}$  can be directed to a desired path. Photonic switching of RF signals is thus realized.

The major parameters of the devices used in the experiment are as follows. The pump and the probe are generated by Agilent N7714A tunable laser source with a wavelength stability of 2.5 pm; the MZM (Fujitsu FTM7938EZ-A) has a bandwidth of 40 GHz and a half-wave voltage of 2.1 V; the SOA (Kamelian SOA-NLL1-C-FA) has a gain recovery time of 25 ps and a polarization dependent gain of less than 1 dB; the PD has a bandwidth of 50 GHz and a responsivity of 0.65 A/W. The RF signal is generated by a vector signal generator (Agilent E8267D). The switched signal is measured and analyzed by a signal analyzer (Agilent N9030A), and the optical spectrum is monitored by an optical spectrum analyzer (OSA) (Yokogawa AQ6370C) with a resolution of 0.02 nm.

## 3. Experiment results and discussion

In the first step, the influences of the key parameters of the proposed photonic microwave switching system are investigated in order to optimize the system performance. The wavelengths of the pump signal and the probe signal are set to be 1555 nm and 1547.79 nm, respectively. A 50-Mbaud 16-QAM RF signal centered at 19 GHz with a power of 6 dBm is modulated on the pump light. Fig. 2 shows the effect of the probe and pump powers on the error vector magnitude (EVM) performance when the SOA bias current

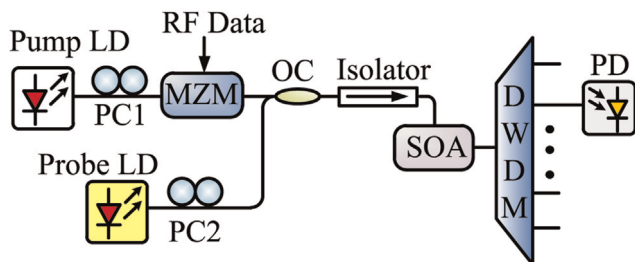


Fig. 1. Experimental setup of photonic switching of RF signals based on XGM in a SOA. LD: laser diode; PC: polarization controller; MZM: Mach-Zehnder modulator; OC: optical coupler; SOA: semiconductor optical amplifier; DWDM: dense wavelength division multiplexing; and PD: photodetector.

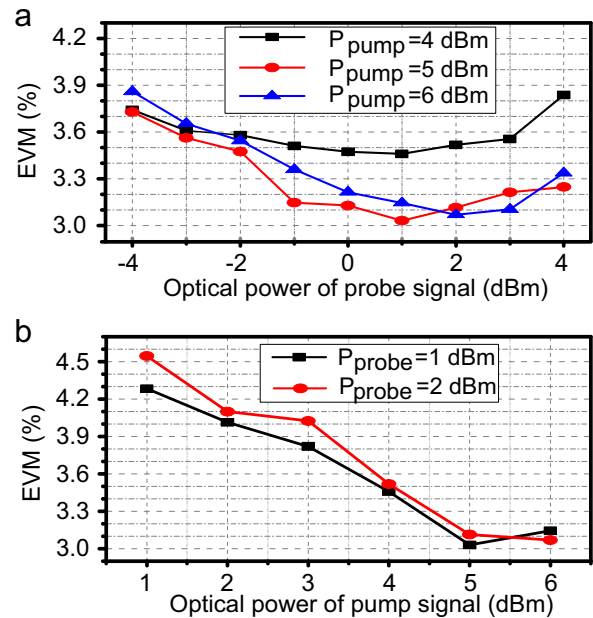
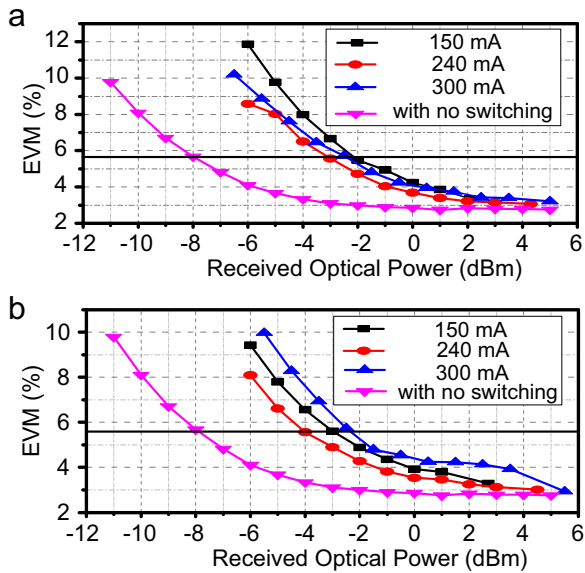


Fig. 2. (a) EVM versus probe power for different pump powers and (b) EVM versus pump power for different probe powers.

is fixed at 240 mA. The EVM values versus the probe power are shown in Fig. 2(a), for pump powers of 4, 5, and 6 dBm, respectively. As can be seen, for each pump power, there exists an optimum probe power with which the EVM has the smallest value. If the probe power is lower than the optimum power, the smaller the probe power is, the worse the EVM will be, since the optical signal-to-noise ratio is reduced with the decreased probe power. When the probe power is higher than the optimum power, the increasing probe power leads to a decreasing EVM value. We attribute this phenomenon to the gain saturation in the SOA which degrades again the optical signal-to-noise ratio. In order to obtain the optimum combination of the pump power and the probe power, EVM values versus the pump powers are also measured when the probe powers is fixed at 1 and 2 dBm, respectively, as shown in Fig. 2(b). The best EVM values are achieved when the pump powers are 5 dBm (for the probe power of 1 dBm) and 6 dBm (for the probe power of 2 dBm), respectively.

Fig. 3 shows the EVMs versus the received optical power at different bias currents of the SOA. The pump and probe powers are fixed at 6 and 2 dBm, or 5 and 1 dBm, respectively. The back-to-back EVM curves without the photonic microwave switching are also measured. As can be seen, for each SOA bias current, the power penalty, defined as the increase in the received optical power to maintain the same EVM value (5.6% for the 16-QAM signal used here [23]) due to the optical switching, in the condition of 5-dBm pump power and 1-dBm probe power is generally lower than that in the condition of 6-dBm pump power and 2-dBm probe power. The smallest power penalty performance is achieved when the SOA bias current is 240 mA in both conditions, i.e. 3.91 dB for the 5-dBm pump power and 1-dBm probe power case, and 4.86 dB for the 6-dBm pump power and 2-dBm probe power case. To explain why the best SOA bias current is 240 mA, the amplified spontaneous emission (ASE) spectra of the SOA at different bias currents are measured, with the results shown in Fig. 4. As can be seen, the lowest ASE noise level is achieved when the bias current is 240 mA, which agrees well with the measured results in [14]. Based on the experimental observation, we can see that the best performance of the XGM-based photonic microwave switch can be achieved when the SOA bias current is 240 mA, the pump power is 5 dBm and the probe power is 1 dBm. Fig. 5 shows



**Fig. 3.** EVM versus the received optical power for 50-Mbaud 16-QAM 19-GHz RF signal without and with switching in the conditions of (a) 1555-nm 6-dBm pump signal and 1547.79-nm 2-dBm probe signal and (b) 1555-nm 5-dBm pump signal and 1547.79-nm 1-dBm probe signal.

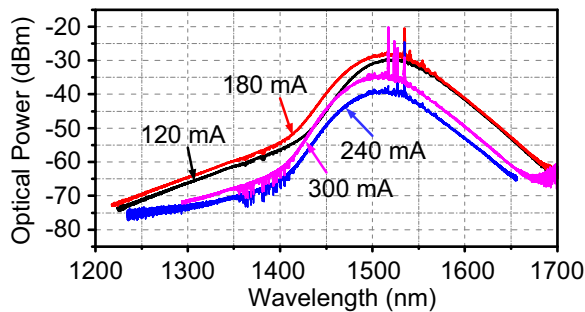


**Fig. 4.** The amplified spontaneous emission (ASE) spectra for SOA bias currents of 120, 180, 240 and 300 mA.

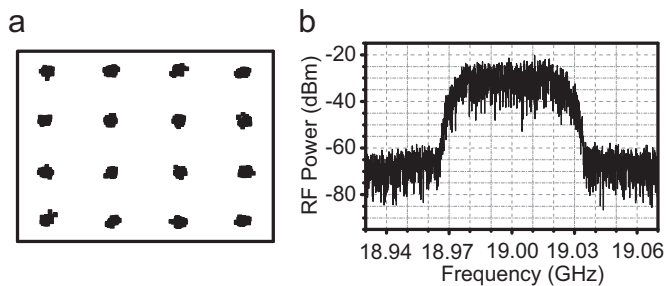


**Fig. 5.** (a) The constellation diagram and (b) electrical spectrum of the switched RF signal under the optimized settings.

the constellation diagram and electrical spectrum of the switched signal with an EVM of 3% under these optimized settings, showing a good performance after switching.

The polarization sensitivity of the photonic microwave switching scheme is also investigated. With the EVM of the RF signal evaluated by 500 symbols being 3.6%, by tuning PC1 in the pump branch to adjust the polarization state of the pump signal, the variation of the EVM is within 0.7%, while the RF output power variation is less than 1 dB. By changing the polarization state of the probe light through adjusting PC2, the variation of the EVM is within 0.3%, and the variation of the RF output power is less than 0.6 dB. The experimental results show that the photonic RF

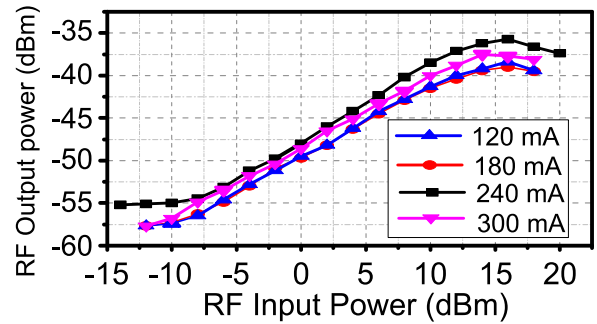


**Fig. 6.** The 19-GHz RF output power versus the RF input power at different SOA bias currents with 5-dBm 1555-nm pump signal and 1547.79-nm 1-dBm probe signal.

switching scheme based on the XGM in a SOA is almost polarization insensitive.

Linearity is another important parameter of the photonic RF switching. With 1555-nm 5-dBm pump signal and 1547.79-nm 1-dBm probe signal, Fig. 6 shows the 19-GHz single-tone RF output power versus the RF input power when the SOA bias current is fixed at 120, 180, 240 or 300 mA. We can see that with 240-mA bias current, the RF output power is the highest at the same RF input power, i.e. the switching efficiency is the highest. The linear working range of the RF input power is about 19 dB, from  $-6$  dBm to about 13 dBm, for the 19-GHz RF signal. The upper bound is restricted mainly by the sinusoidal transfer function of the MZM, while the lower bound is existed because of the relatively large noise introduced by the SOA. Fixing the SOA bias current at 240 mA, we also measured the EVM performance as a function of the input RF power when the 19-GHz signal is used to carry a 50-Mbaud 16-QAM signal, with the results shown in Fig. 7. Applying the EVM threshold of 5.6% for 16-QAM signal, the dynamic range of the RF input power is about 17.09 dB.

Two-tone measurements are used to further analyze the linearity of the photonic microwave switching. Two 19-GHz sine waves separated by 10 MHz with 6-dBm power are generated by Agilent 8267D and injected into the photonic microwave switch. The output tones at the two frequencies as well as the in-band third-order intermodulation (IMD3) tones are measured over a range of input powers to obtain the spurious-free dynamic range (SFDR). The SFDR performances without and with optical microwave switching at different SOA bias currents are shown in Fig. 8. The noise floor without the optical microwave switching is measured to be  $-161.83$  dBm, while the values with the optical microwave switching are  $-164.05$ ,  $-163.19$ ,  $-157.42$ , and  $-158.92$  dBm for the SOA bias currents of 120, 180, 240, 300 mA, respectively. Without the optical microwave switching, the SFDR is  $96.43$  dB Hz<sup>2/3</sup>. At the SOA bias currents of 120, 180, 240 and 300 mA, the SFDRs after optical microwave switching change to be 86.85, 88.19, 86.32 and 87.82 dB Hz<sup>2/3</sup>, respectively. We can see that the lowest penalty of SFDR is about 8.24 dB when the bias currents are 180 mA. For the condition with 240-mA SOA bias current, the switching penalty of SFDR is 10.11 dB.

An important feature for the photonic RF switching is the uniform channel-performances for both up- and down-converted signals in the wavelength domain. Fig. 9(a), (b) and (c) show the RF output power, the EVM performance and the SFDR of the photonic microwave switching versus the wavelength of the probe signal for both up- and down-conversion with 240-mA SOA bias current, respectively. The SFDR values are all measured considering the measured noise floor of  $-157.42$  dBm for the 240-mA SOA bias current condition. A 50-Mbaud 16-QAM RF signal centered at 19 GHz with a power of 6 dBm is modulated on the 5-dBm optical pump signals. The wavelength of the pump signal is set to be 1555 nm for the down-conversion measurement and 1545 nm for

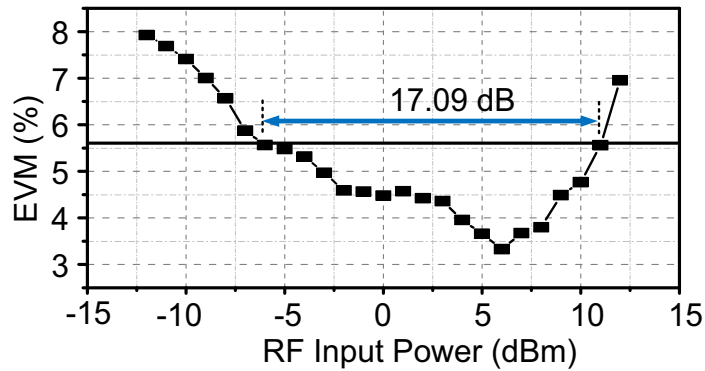


Fig. 7. The EVM as a function of the input power of the 50-Mbaud 16-QAM signal centered at 19 GHz when the SOA bias current is 240 mA, and the powers of the 1555-nm pump signal and 1547.79-nm probe signal are 5 and 1 dBm, respectively.

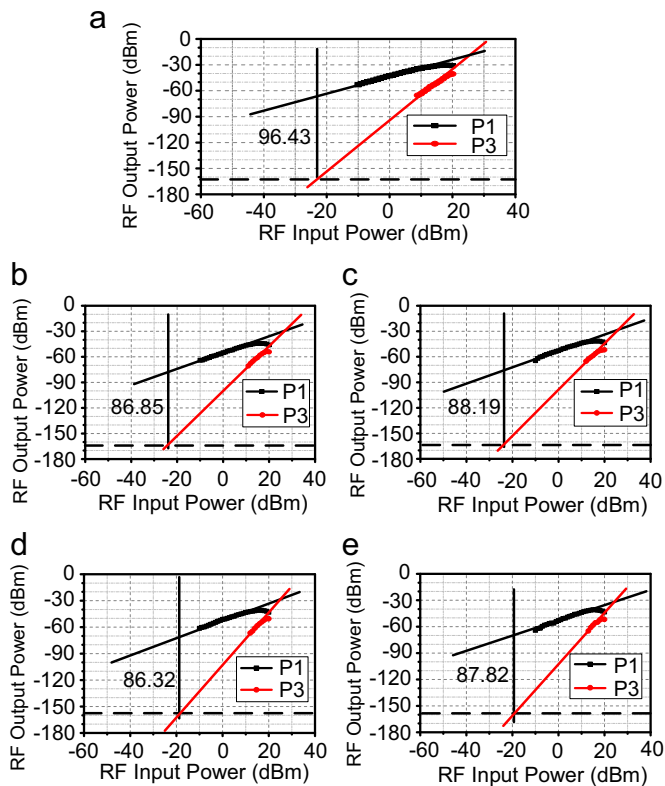


Fig. 8. The linearity performance of spurious-free dynamic range (SFDR) (a) with no optical microwave switching; with optical microwave switching with 5-dBm 1555-nm pump signal and 1547.79-nm 1-dBm probe signal at SOA bias currents of (b) 120 mA (c) 180 mA (d) 240 mA and (e) 300 mA.

the up-conversion measurement, respectively. The channel difference of the RF output power is about 2.04 dB for down-conversion and 1.47 dB for up-conversion. The variation of the EVM value among different channels is 0.286% and 0.177% for down-conversion and up-conversion, respectively. The SFDR difference is about 5.28 dB for up-conversion and 2.44 dB for down-conversion. Thus it can be seen that the RF output power (representing the switching efficiency), the EVM performance, and the SFDR of the photonic microwave switching scheme show good uniformity for both up- and down-conversion.

In addition, the high switching speed is also an important feature for the practical applications. For the proposed photonic microwave switching based on XGM effect, the switching time is mainly limited by the carrier recovery time of the SOA, which is about several hundred picoseconds [22]. Thus the switching time is also in the order of hundred picoseconds. With this fast

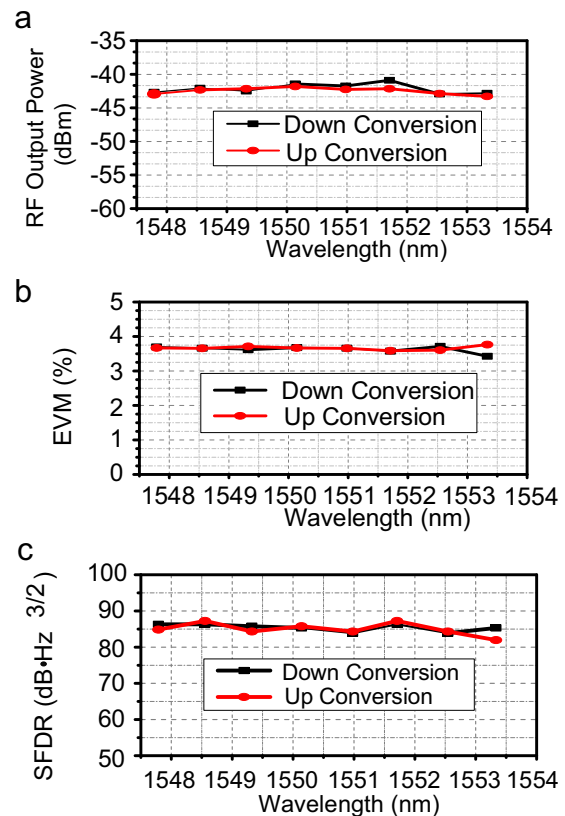


Fig. 9. (a) RF output power, (b) EVM and (c) the SFDR values of the photonic microwave switching versus the wavelength of the probe signal with 240-mA SOA bias current, 5-dBm pump signal of 1555 nm for down-conversion and 1545 nm for up-conversion.

switching feature, the XGM-based SOA can be used in applications where GHz switching speed is required. In addition, several methods have been proposed to speed up the carrier recovery to further increase the switching speed, e.g. the use of a holding beam [24].

#### 4. Conclusions

Photonic microwave switching is one of key technologies to realize signal routing, function switching or system reconfiguration in microwave system. We have experimentally investigated the performance of the photonic microwave switching based on the XGM effect in a SOA. For a single channel switching, the influences of the optical power of the pump and probe signals, the

SOA bias current and the modulation depth on the EVM penalty are analyzed and discussed. Optimum probe power, pump power, SOA bias current and modulation depth are obtained. The linearly working range of the RF input power is about 17.09 dB. The SFDR performance is analyzed for single-channel switching. An optimum linearity penalty of about 8.24 dB is observed. The polarization-insensitivity due to the low polarization dependence of the SOA is also confirmed. Channel uniformities which are important for the photonic microwave switching applications are also investigated. The switching efficiency and the EVM performances have good uniformities for both up- and down- switched signals. Good channel uniformity can also be found for the SFDR performance of the photonic microwave switching. The channel uniformity opens the possibility of using photonic microwave switching to realize the function switching and system re-configurability in arrayed systems.

### Acknowledgments

This work was supported in part by the National Natural Science Foundation of China (61201048 and 61422108), the Natural Science Foundation of Jiangsu Province (BK2012381 and BK2012031), the Aviation Science Foundation of China (2013ZC52040).

### References

- [1] G.C. Tavik, C.L. Hilterbrick, J.B. Evins, J.J. Alter, J.G. Crnkovich Jr, J.W. de Graaf, W. Habicht, G.P. Hrin, S.A. Lessin, D.C. Wu, *IEEE Trans. Microw. Theory Tech.* 53 (2005) 1009.
- [2] M. Sotom, B. Benazet, A.L. Kerneq, M. Maignan, *Proceedings of ECOC*, 2009, paper 10.16.13.
- [3] I.-S. Joe, O. Solgaard, *Proceedings of AVFOP*, 2005, paper TuA1.
- [4] E. Brookner, *Proceedings of IEEE Radar*, 2007, p. 37.
- [5] S.L. Pan, D. Zhu, F.Z. Zhang, *Trans. Nanjing Univ. Aeronaut. Astronaut.* 31 (2014) 219.
- [6] Y. Vlasov, W.M. Green, F. Xia, *Nat. Photonics* 2 (2008) 242.
- [7] S. Hernandez, M. Zahir, F. Filhol, L. Marchand, *Proceedings of SPIE MOEMS and Miniaturized Systems IX*, 2010, p. 75940S.
- [8] F. Chen, D. Yao, *Opt. Commun.* 312 (2014) 143.
- [9] G.I. Papadimitriou, C. Papazoglou, A.S. Pomportsis, *J. Lightw. Technol.* 21 (2003) 384.
- [10] G. Coppola, L. Sirlito, I. Rendina, M. Iodice, *Opt. Eng.* 50 (2011) 071112.
- [11] K. Cui, X. Feng, Y. Huang, Q. Zhao, Z. Huang, W. Zhang, *Proceedings of SPIE Optoelectronic Interconnects XIII*, 2013, p. 863018.
- [12] Y.F. Yan, C.T. Zheng, L. Liang, J. Meng, X.Q. Sun, F. Wang, D.M. Zhang, *Opt. Commun.* 285 (2012) 3758.
- [13] L. Chen, *Proceedings of Photonics in Switching*, 2014, paper PM2C.1.
- [14] X. Qian, P. Hartmann, S. Li, R.V. Penty, I.H. White, *Proceedings of MWP*, 2005, p. 317.
- [15] M. Crisp, E.T. Aw, A. Wonfor, R.V. Penty, I.H. White, *Proceedings of OFC/NFOEC*, 2008, paper OThP4.
- [16] H.-D. Jung, M. Presi, P. Choudhury, T. Ditewig, E. Tangdiongga, E. Ciaramella, T. Koonen, *Proceedings of ECOC*, 2010, paper, P6.16.
- [17] H. Jung, N. Calabretta, E. Tangdiongga, H. Dorren, A. Koonen, *Proceedings of ECOC*, 2008, paper, Tu.4.F.2.
- [18] H. Yang, Y. Shi, C. Okonkwo, E. Tangdiongga, A. Koonen, *Proceedings of MWP*, 2010, p. 181.
- [19] H.-D. Jung, C. Okonkwo, E. Tangdiongga, T. Koonen, *Proceedings of ECOC*, 2009, paper 4.5.3.
- [20] T. Durhuus, B. Mikkelsen, C. Joergensen, S.L. Danielsen, K.E. Stubkjaer, *J. Lightw. Technol.* 14 (1996) 942.
- [21] D. Zhu, H. Wu, S.L. Pan, *Proceedings of ICOCN*, 2014.
- [22] S.-J. Chua, B. Li, Elsevier, 2010.
- [23] *IEEE Std.* 802. 11 a/b/g (1997/1999/2003).
- [24] M.T. Hill, E. Tangdiongga, H. De Waardt, G. Khoe, H. Dorren, *Opt. Lett.* 27 (2002) 1625.